Acta Pharmaceutica Sinica B 2026;16(7):4442−4458

Chinese Pharmaceutical Association
Institute of Materia Medica, Chinese Academy of Medical Sciences

Acta Pharmaceutica Sinica B

www.elsevier.com/locate/apsb
www.sciencedirect.com

ORIGINAL ARTICLE

Acquired pharmacoresistance in temporal lobe epilepsy is driven by $Na_v1.6$-mediated subicular hyperexcitability

Yuanzhi Yang[a,†], Menghan Li[a,†], Minjuan Sun[a,†], Shuo Zhang[a,b,†], Xiongfeng Guo[a,†], Shuangshuang Wu[a], Yiwei Gong[a], Lan Huang[a], Tong Liu[a], Junxiu Ye[a], Xiangyu Ma[a], Xiaoyun Qiu[a], Shuang Wang[c], Fan Fei[a], Yu Du[a], Yi Wang[a], Zhong Chen[a,*], Cenglin Xu[a,*]

[a]*Zhejiang Collaborative Innovation Center for the Brain Diseases with Integrative Medicine, Zhejiang Key Laboratory of Neuropsychopharmacology, Huzhou Central Hospital, The Fifth School of Clinical Medicine of Zhejiang Chinese Medical University, School of Pharmaceutical Science, Zhejiang Chinese Medical University, Hangzhou 310053, China*
[b]*Department of Pharmacy, The First Affiliated Hospital of Zhejiang Chinese Medical University (Zhejiang Provincial Hospital of Chinese Medicine), Hangzhou 310006, China*
[c]*Epilepsy Center, Second Affiliated Hospital, School of Medicine, Zhejiang University, Hangzhou 310050, China*

Received 22 May 2025; received in revised form 29 August 2025; accepted 4 November 2025

KEY WORDS

Anti-seizure medication;
Hyperexcitability;
$Na_v1.6$;
Pharmacoresistance;
Pyramidal neurons;
Sodium channel;
Subiculum;
Temporal lobe epilepsy

Abstract Pharmacoresistance to anti-seizure medications (ASMs) remains a major unmet challenge in temporal lobe epilepsy (TLE), and occurs diversely, as classified to primary or acquired manner. The pathophysiological underpinnings of acquired pharmacoresistance remain elusive. Here, using a hippocampal kindling mouse model, we established that prolonged lamotrigine (LTG) treatment—either during or after kindling—induces broad-spectrum resistance to multiple ASMs, effectively recapitulating clinical patterns of acquired pharmacoresistance. Multimodal interrogation revealed hyperexcitability of subicular pyramidal neurons as a critical factor in pharmacoresistance, characterized by elevated c-Fos expression specifically within the subiculum, as well as hyperexcitability of subicular glutamatergic pyramidal neurons. This hyperexcitability phenotype stemmed from $Na_v1.6$ upregulation, driving both enhanced persistent sodium current (I_{NaP}) and a pro-excitatory shift in voltage-dependent activation kinetics of voltage-gated sodium channel (VGSC). Crucially, pharmacological activation of subicular $Na_v1.6$

*Corresponding authors.
E-mail addresses: chenzhong@zju.edu.cn (Zhong Chen), xucenglin5zz@zju.edu.cn (Cenglin Xu).
[†]These authors made equal contributions to this work.
Peer review under the responsibility of Chinese Pharmaceutical Association and Institute of Materia Medica, Chinese Academy of Medical Sciences.

https://doi.org/10.1016/j.apsb.2026.04.011

sufficed to induce acquired pharmacoresistance in pharmaco-responsive mice. Conversely, subiculum-specific $Na_v1.6$ knockdown in pyramidal neurons (but not GABAergic neurons) prevented or reversed pharmacoresistance, while analogous genetic manipulation in the CA1 had no such impact. Chemogenetic inhibition of subicular pyramidal neurons (mimicking ASM effects) restored drug responsiveness, directly implicating compensatory increases in $Na_v1.6$ offsetting ASM's inhibitory function on subicular excitability in acquired pharmacoresistance. These findings collectively identify $Na_v1.6$ upregulation in subicular pyramidal neurons as a critical driver of acquired pharmacoresistance in TLE, highlighting a novel therapeutic target for refractory epilepsy.

1. Introduction

Pharmacoresistance persists as a paramount therapeutic obstacle in epilepsy, ranked among the top five most burdensome neurological disorders[1]. Alarmingly, over 30% of epilepsy patients develop pharmacoresistance[2], enduring uncontrolled seizures that amplify risks of life-threatening complications and profound psychosocial burdens[3]. Clinically, pharmacoresistance in epilepsy manifests through two distinct temporal phenotypes: innate pharmacoresistance characterized by immediate therapeutic failure upon anti-seizure medication (ASM) initiation; and acquired pharmacoresistance marked by progressive loss of drug efficacy following an initial response period[4-6]. This dichotomy holds particular clinical significance in temporal lobe epilepsy (TLE), where acquired pharmacoresistance ($\sim$60% of cases) associates with more extensive mesial temporal sclerosis and complex epileptogenic networks compared to innate presentations ($\sim$40%)[7,8]. Building on these clinical observations, emerging translational evidence underscores a critical pathophysiological link between epileptogenic network remodeling and pharmacoresistance development[9]. Unlike innate pharmacoresistance which is often correlated with obvious indicators (such as hippocampal sclerosis), the insidious progression of acquired pharmacoresistance creates critical diagnostic dilemmas, including delayed recognition of therapeutic failure and missed opportunities for early intervention[2]. Elucidating the neural circuit/molecular drivers of acquired pharmacoresistance is thus imperative for developing mechanism-based strategies to counteract this treatment-refractory state.

The hippocampal subiculum has been demonstrated to orchestrate epileptic hyperexcitability through its glutamatergic pyramidal neuron networks[10]. Crucially, *in vitro* electrophysiological recordings from resected hippocampal specimens of pharmacoresistant TLE patients revealed synchronized epileptiform discharges localized specifically to the subiculum[11]. Our longitudinal studies in TLE model further demonstrate that subicular pyramidal neurons govern both hippocampal seizure propagation and innate pharmacoresistance through network-level dysregulation[8,10,12-15]. Whether subicular neuronal hyperactivity is also a principal mechanism in acquired pharmacoresistance, an area that has received minimal investigation despite its importance, and whose molecular underpinnings worth to be further elucidated.

Voltage-gated sodium channel (VGSC) dysregulation constitutes a fundamental mechanism underlying neuronal hyperexcitability in epilepsy[16]. Among VGSC isoforms, $Na_v1.6$-enriched at the axon initial segment (AIS)-plays a pivotal role in epileptogenesis. Human and animal studies demonstrate that *SCN8A* (encoding $Na_v1.6$) gain-of-function mutations as causative in developmental and epileptic encephalopathies[17], while whole-brain $Na_v1.6$ knockdown suppresses seizure susceptibility and kindling progression in rodents[18]. Intriguingly, mice with chronic TLE spontaneous seizures exhibit $Na_v1.6$-mediated hyperexcitability in subicular pyramidal neurons[19]. However, the potential contribution of $Na_v1.6$ to pharmacoresistance mechanisms, particularly within epileptogenic hubs like the subiculum remains unexplored.

Here, through multimodal interrogation of an acquired pharmacoresistant TLE model, we present the first evidence that subiculum-specific $Na_v1.6$ upregulation drives acquired pharmacoresistance *via* enhanced hyperexcitability of pyramidal neuron, establishing $Na_v1.6$ as a dual-purpose target for both preventing and reversing acquired pharmacoresistance in TLE.

2. Materials and methods

2.1. Animals

Given our previous studies have confirmed that sex would not significantly influence the pharmacoresistant TLE phenotypes in rodents[8], we used male C57BL/6J mice (10-week-old, SLAC Laboratory) and transgenic strains (*CaMKIIα-Cre*: JAX 005539; *Vgat-Cre*: JAX 016962) in the current study. All mice were maintained under 12-h light/dark cycles with ad libitum access to food/water.

2.2. Hippocampal kindling model of acquired pharmacoresistant TLE

According to our previous studies[20,21], anesthetized mice were stereotaxically implanted with bipolar electrodes in the right CA3 (AP −2.9, ML −3.0, DV −3.0 mm). After 7-day recovery, afterdischarge threshold (ADT) was determined using 20 Hz biphasic pulses (1 ms/pulse, 2 s duration)[22]. Kindling was achieved through daily stimulations (6 times per day, 400 μA, 1 s) until three consecutive Racine's stage 5 seizures[23]. Acquired pharmacoresistance was induced and validated through two sequential paradigms[20,24,25]: (1) During the kindling process, mice received subtherapeutic doses of ASMs administered intraperitoneally three times daily, including lamotrigine (LTG, 5 mg/kg), carbamazepine (CBZ, 7 mg/kg), or levetiracetam (LEV, 7 mg/kg). The first administration was delivered 30 min prior to the initial kindling stimulation, followed by subsequent administration immediately after the 2nd and 4th stimulations. Vehicle control groups received equivalent volumes of saline. (2) When full

kindled, mice were challenged with therapeutic doses of ASMs (LTG: 15 mg/kg; CBZ: 20 mg/kg; LEV: 20 mg/kg; valproate acid [VPA]: 200 mg/kg; rufinamide [RUF]: 50 mg/kg; phenytoin [PHT]: 50 mg/kg), with seizure severity reassessed 30 min post-injection. Pharmacoresistance was defined as persistent secondary generalized seizures (Racine's stages 4 and 5) following ASM administration. Once the seizure stage was reduced to $\leq$3 by any ASM treatments, we deemed this trial was effective[26]. The stage-lowered ratio (obtained by calculating the ratio of the difference in seizure stages before and after ASMs to the baseline stages) and effective rate of each ASM was also compared among different groups.

2.3. Viral injection

To achieve region-specific $Na_v1.6$ modulation, *CaMKIIα-Cre* or *Vgat-Cre* mice received stereotaxic injections of *AAV-DIO-EGFP-shRNA* (*SCN8A*) (1.20×10^{13} particles/mL, TargetSeq: ACTCTAACCTGAAGATCTATA) or non-targeting shRNA as control virus *AAV-DIO-EGFP-ShRNA* (NC) (1.27×10^{13} particles/mL). For chemogenetic inhibition, *AAV-DIO-hM4Di-mCherry* (2.36×10^{12} particles/mL) was selected, and *AAV-DIO-mCherry* (3.32×10^{12} particles/mL) was selected as control virus for chemogenetic experiments. All viruses were purchased from Obio Technology Co., Ltd. (Shanghai, China). Viral suspensions (0.8 μL) were infused into the right subiculum (AP −3.4 mm; ML −2.0 mm; DV −1.8 mm) or CA1 (AP −2.0 mm; ML −1.3 mm; DV −1.6 mm) using a microsyringe pump (0.1 μL/min flow rate; 5-min post-injection stabilization). Behavioral tests commenced after 3-week viral expression.

2.4. Pharmacological activation of $Na_v1.6$ in the subiculum

For targeted pharmacological $Na_v1.6$ activation, a guide cannula was stereotactically implanted into the right subiculum. $Na_v1.6$ agonist Veratridine (VET; 1 or 5 μmol/L in 150 nL)[27], was subsequently microinfused through an internal injection cannula connected to an infusion pump (Harvard Apparatus, model 70-4507). The infusion was performed at a controlled rate of 30 nL/min to ensure precise local delivery while minimizing tissue damage.

2.5. In vitro electrophysiology

Electrophysiological recordings were performed as previously described[8,13]. Acute hippocampal slices (300 μm) were prepared in ice-cold oxygenated artificial cerebrospinal fluid (ACSF) (in mmol/L: 125 NaCl, 3.5 KCl, 1.25 NaH_2PO_4, 0.5 $MgCl_2$, 26 $NaHCO_3$, 25 glucose, and 1 $CaCl_2$). Current-clamp recording was obtained from subicular pyramidal neurons using glass pipettes (3−5 MΩ) filled with intracellular solution (in mmol/L: 140 K-gluconate, 5 NaCl, 2 Mg-ATP, 0.2 EGTA, and 10 HEPES). Neuronal excitability was assessed by injecting stepped currents (−200 to +300 pA, 20 pA increments, 500 ms duration) to elicit action potentials (AP). Voltage-clamp recording of sodium currents was performed using an intracellular solution (in mmol/L: 140 CsF, 2 $MgCl_2$, 1 EGTA, 10 HEPES, 4 Na_2ATP, and 0.3 NaGTP). For transient Na^+ currents, cells were stepped from −100 mV to +20 mV (10 mV increments). $Na_v1.6$-mediated persistent sodium currents (I_{NaP}) were isolated in tetrodotoxin-free conditions using voltage ramps (−100 mV to −10 mV, 65 mV/s) with bath solution (in mmol/L: 30 NaCl, 120 TEA-Cl, 10 $NaHCO_3$, 1.6 $CaCl_2$, 2 $MgCl_2$, 0.2 $CdCl_2$, 5 4-AP, and 15 Glucose). All recordings were performed using an EPC10 amplifier (HEKA Instruments, Stuttgart, Germany) with PatchMaster software (HEKA Instruments, Stuttgart, Germany).

2.6. Immunohistochemistry

Mice underwent transcardial perfusion with ice-cold saline followed by 4% paraformaldehyde (PFA) in 0.1 mol/L phosphate buffer (PB, pH 7.4) under deep anesthesia. For c-Fos analysis, animals were sacrificed 90 min post-behavioral testing to capture peak protein expression. Coronal sections (25 μm) obtained with the freezing microtome were incubated with primary antibodies: c-Fos (1:1000 in working dilution, Abcam ab208942), GABA (1:500, Sigma−Aldrich A2052) or $Na_v1.6$ (1:200 in working dilution, Abcam ab65166) overnight at 4 °C. $Na_v1.6$-stained sections were subsequently probed with CaMKIIα antibody (1:200 in working dilution, Proteintech 66843-1-Ig) for neuronal subtype verification.

2.7. Immunoblot

Subicular tissues homogenized in RIPA buffer were subjected to SDS-PAGE (40 μg/lane). Differential transfer conditions were applied: 107 V for 1 h (β-actin) *vs* 2.5 h ($Na_v1.6$), due to the molecular weight of $Na_v1.6$ (∼250 kDa) being significantly higher than that of β-actin (∼42 kDa). Membranes were probed with anti-$Na_v1.6$ (Abcam ab65166; 1:200 in working dilution) and

Table 1 The PCR primers of subunits of voltage-gated sodium channels.

Gene/Protein	PCR primers
SCN1A ($Na_v1.1$)	f.p. 5′-TGGTGTCGGAGCCTCTGGAG-3′, r.p. 5′-GGCGGAGGTGGCACTGAAC-3′
SCN2A ($Na_v1.2$)	f.p. 5′-AAGAGCAGGCTGGAGAGGAAGAG-3′, r.p. 5′-TCAAGAGAGACTGGTGTGGAGAGG-3′
SCN8A ($Na_v1.6$)	f.p. 5′-GGTGTTCTGCCTGAGTGTCTTCG-3′, r.p. 5′-AGCCTCTGGTGCCGTTCTCC-3′
SCN1B ($Na_v\beta1$)	f.p. 5′-CAACACCAGCGTCGTCAAG-3′, r.p. 5′-TCTGAGGCGTTCTCTTGTGC-3′
SCN2B ($Na_v\beta2$)	f.p. 5′-GCAGCTAGAAGACGAAGGCA-3′, r.p. 5′-GACCACIATCAGCACCAAGA-3′
SCN3B ($Na_v\beta3$)	f.p. 5′-CACTGAAGAGGCGGGAGAAG-3′, r.p. 5′-TGAAGGGATAGCAAGGTAGTCAG-3′

f.p., forward primer; r.p., reverse primer.

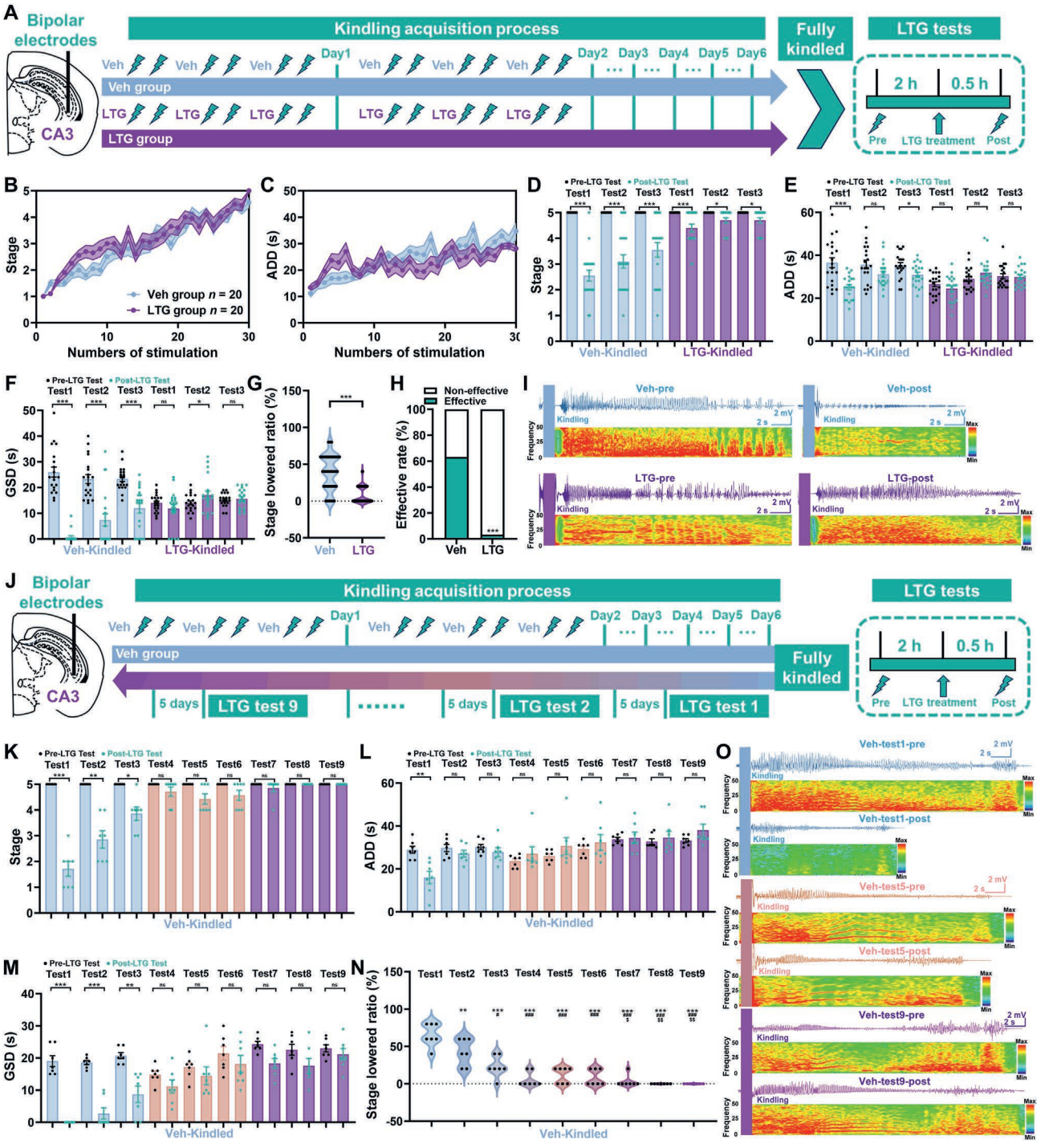

Figure 1 Long-term lamotrigine administration induces acquired pharmacoresistance. (A) Establishment of the acquired pharmacoresistant TLE model. LTG was co-administrated during the hippocampal kindling process, when the mice were fully kindled, the anti-seizure efficacy was evaluated in mice receiving LTG (the LTG-Kindled group) or vehicle treatment (the Veh-Kindled group). (B, C) Comparative progression of seizure stages and ADDs during the kindling process of the two groups ($n = 20$ for each group). (D−F) Effect of LTG on the seizure stages (D), ADDs (E) and GSDs (F) in fully kindled mice from the two groups ($n = 20$ for each group; post-LTG test *vs* pre-LTG test for each test was performed; for seizure stages, $^*P < 0.05$, $^{***}P < 0.001$, non-parametric Mann−Whitney test; for ADDs and GSDs, $^*P < 0.05$, $^{***}P < 0.001$, paired *t*-test). (G) The comparison of stage lowered ratio caused by LTG between the two groups ($^{***}P < 0.001$, paired *t*-test). (H) The comparison of the effective rate of LTG between the two groups ($^{***}P < 0.001$, χ^2 test). (I) The representative seizure EEG and spectrums during the LTG test on fully kindled mice from the two groups. (J) The experimental design of examining the long-term impact of LTG administration on its anti-seizure efficacy. A total of nine LTG tests were performed on the fully kindled mice from the Veh-Kindled group with 5-day intervals. (K−M) The efficacy of LTG on the seizure stages (K), ADDs (L) and GSDs (M) of the fully kindled mice from the Veh-Kindled groups ($n = 7$, post-LTG test *vs* pre-LTG test for each test was performed; for seizure stages, $^*P < 0.05$, $^{**}P < 0.01$, $^{***}P < 0.001$, non-parametric Mann−Whitney test; for

β-actin (Proteintech 66009-1; 1:5000 in working dilution), followed by species-matched HRP-conjugated secondaries (Multi Sciences; 1:3000 in working dilution). Densitometric analysis used Quantity-One software (Bio-Rad).

2.8. Real time polymerase chain reaction (RT-PCR)

Total RNA extracted from microdissected subiculum with Trizol was reverse-transcribed into cDNA. VGSC isoform expression was quantified using SYBR Green on a real-time cycler with specific primers (Table 1).

2.9. Statistics

Data expressed as mean ± standard error of mean (SEM) were analyzed using GraphPad Prism 9.1.1. The number of experimental replicates (n) was indicated in the Figure legend, and referred to the number of experimental subjects in each experimental condition. The appropriate statistical methods were indicated in the Figure legend, respectfully.

3. Results

3.1. Chronic LTG administration induced acquired pharmacoresistance

Expanding on prior observations of LTG-induced pharmacoresistance[20,24,25,28], we systematically investigated this phenomenon in hippocampal-kindled mice *via* co-administration of LTG during kindling process (Fig. 1A). While LTG pretreatment did not alter kindling acquisition, indicated by the comparable seizure stage progression (Fig. 1B) and after-discharge durations (ADDs, Fig. 1C) with vehicle controls, it induced robust pharmacoresistance upon subsequent therapeutic challenge (15 mg/kg): LTG effectively suppressed seizure stages, shortened ADDs and reduced generalized seizure durations (GSD) in Veh-kindled controls, but showed minimal efficacy in LTG-pretreated mice (LTG-kindled, Fig. 1D−F). Quantitative examination revealed significantly reduced stage-lowered ratios and effective rates in LTG-kindled mice caused by LTG (Fig. 1G and H), corroborated by EEG spectral analyses (Fig. 1I). To validate whether the acquired pharmacoresistance persists under sustained LTG treatments, 4 weeks of sustained daily LTG treatment (15 mg/kg) were employed on mice from the LTG-kindled group, followed by a re-evaluation of LTG's anti-seizure efficacy. As denoted in Supporting Information Fig. S1A−S1D, we confirmed a stale lack of anti-seizure efficacy of LTG even after sustained LTG treatment. This demonstrates that the acquired pharmacoresistance phenotype is non-transient and persists under prolonged ASM exposure, validating the robustness and chronic nature of our model.

To assess whether sustained therapeutic LTG exposure drives acquired pharmacoresistance in initially drug-responsive mice, we administered nine consecutive LTG challenges (15 mg/kg) to fully kindled mice from the Veh-kindled group (Fig. 1J). Progressive therapeutic failure emerged across successive administrations, evidenced by declining efficacy in seizure stage reduction, ADD suppression, and GSD attenuation (Fig. 1K−M). Stage-lowered ratios progressively diminished from initial to final tests (Fig. 1N), with representative EEGs and spectra confirming the gradual loss of LTG efficacy (Fig. 1O). These findings establish that chronic LTG treatment induces acquired pharmacoresistance in fully kindled mice.

3.2. Subicular pyramidal neuron hyperexcitability mediated by $Na_v1.6$ upregulation in pharmacoresistant TLE mice

To identify key brain regions underlying acquired pharmacoresistance, c-Fos mapping was performed after experiencing seizures in both groups, and it revealed subiculum-specific hyperactivity in LTG-treated mice (Fig. 2A). Notably, the subiculum showed significantly stronger c-Fos fluorescence intensity in the LTG group compared with the Veh group, while other hippocampal subfields showed only nonsignificant or weaker activation trends (Supporting Information Fig. S2A−S2D). Specifically, the number of subicular *Fos*-positive cells was significantly higher in the LTG group (Fig. 2B and C). Given that subicular pyramidal neurons are the main neuronal type responsible for the initiation and maintenance of epileptic activities[10], we further examined the excitability of subicular pyramidal neurons in the two groups. As indicated by the representative traces (Fig. 2D), subicular pyramidal neurons in the LTG group exhibited a greater number of action potentials (APs) firings elicited by each depolarizing current (Fig. 2E), leading to a significantly lower rheobase current in the LTG group (Fig. 2F). Then we analyzed the basic AP properties of subicular pyramidal neurons. The input resistance and resting membrane potentials of subicular pyramidal neurons were comparable between the two groups (Fig. 2G and H). The threshold of AP exhibited a more hyperpolarizing shift in the LTG group (Fig. 2I). Subicular pyramidal neurons in the LTG group had a shorter decay time and higher amplitude in the first AP elicited by the rheobase current, while the rise time and *tau* value remained comparable (Fig. 2J−M). The maximal negative voltage attained after the completion of repolarization was significantly depolarized in the LTG group compared with the Veh group (Fig. 2N). To further test the repolarization ability, we applied stepped hyperpolarizing currents and found that nearly half of the subicular pyramidal neurons elicited rebound firing of AP caused by the repolarization in the LTG group, while the rate was significantly lower in the Veh group (Fig. 2O). In neurons without rebound firing, the depolarized sag voltage value was higher in the LTG group (Fig. 2P). Taken together, current-clamp recordings indicated that subicular pyramidal neurons were more excitable, and exhibited a stronger recovery from hyperpolarization in pharmacoresistant mice.

Given that VGSC is crucial for the excitability of pyramidal neurons, we further asked whether pro-excitatory alterations in VGSC physiology exist in subicular pyramidal neurons from the LTG group. Representative sodium currents from the two groups were shown in Fig. 2Q. Analysis of current-voltage (I/V) curves revealed a significant hyperpolarizing shift in the $V_{1/2}$ of activation in the LTG group compared with the Veh group (Fig. 2R and S), indicating increased VGSC function in subicular pyramidal

ADDs and GSDs, $^{**}P< 0.01$, $^{***}P< 0.001$, paired t-test). (N) The comparison of stage lowered ratio caused by LTG among each test ($^{**}P< 0.01$, $^{***}P< 0.001$, compared with the Test1; $^{\#}P< 0.05$, $^{\#\#\#}P< 0.001$, compared with the Test2; $^{\$}P< 0.05$, $^{\$\$}P< 0.01$, compared with the Test3; one-way ANOVA followed by Tukey's *post hoc* test). (O) The representative seizure EEGs and spectrums of the first, fifth, and ninth LTG tests. The data are presented by mean ± SEM.

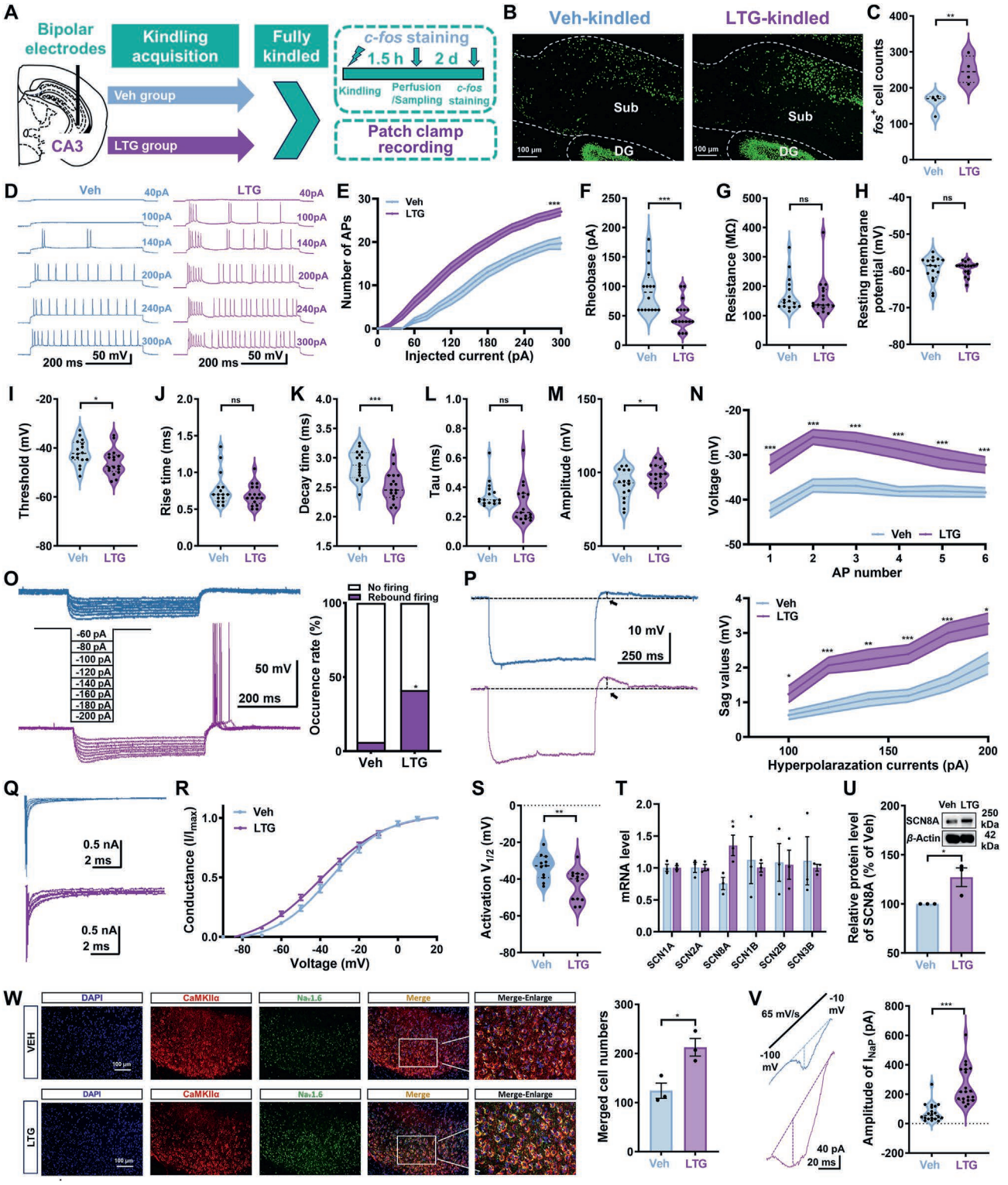

Figure 2 $Na_v1.6$ is increased in hyperexcitable subicular pyramidal neurons in acquired pharmacoresistant mice. (A) The schematic of the experimental procedure, when mice from the two groups were fully kindled, one cohort underwent *c-Fos* immunofluorescence staining at 1.5 h post generalized seizure onset, while the other cohort was used for *in vitro* electrophysiology recordings. (B) The representative *c-Fos* staining image of the subiculum from mice experienced generalized seizures from the two groups. (C) The comparison of the *c-Fos* positive cell counts between the two groups ($n = 4$ slices from 4 mice for each group, $^{**}P < 0.01$, unpaired *t*-test). (D) The representative traces of AP firings of the subicular pyramidal neurons elicited by different depolarized currents from the two groups. (E) The comparison of AP numbers elicited by each stepped current injected into the subicular pyramidal neurons ($n = 16$ from 5 mice for the Veh group, $n = 17$ from 5 mice for the LTG group, $^{***}P < 0.001$, two-way ANOVA test). (F) The comparison of the rheobase of the two groups ($^{***}P < 0.001$, unpaired *t*-test). (G, H) The input resistances and resting membrane potentials were comparable among the two groups. (I–M) The comparison of the basic AP properties between

neurons from the pharmacoresistant TLE mice. This finding led us to further examine the subicular mRNA levels of VGSC subunits between the two groups. Intriguingly, the *SCN8A* mRNA level encodeing $Na_v1.6$ was significantly higher in the LTG group, while other subunits showed no significant changes (Fig. 2T). This observation was verified by WB results showing increased subicular SCN8A protein levels in the LTG group (Fig. 2U). IHC experiments also revealed greater co-expressed of $Na_v1.6$ in subicular pyramidal neurons from the LTG group compared to controls (Fig. 2W). Finally, by recording the persistent sodium currents (I_{NaP}) that were specifically mediated by $Na_v1.6$ in subicular pyramidal neurons (Fig. 2V), we confirmed that the $Na_v1.6$ currents was increased in subicular pyramidal neurons of the LTG group. In line with previous studies, here we have proposed that increased Nav1.6 effectively drive hyper-excitability in subicular pyramidal neurons *via* its unique kinetics[19,29]. However, the increased $Na_v1.6$ in subiculum seemed to be specific in pharmacoresistant TLE mice, as the protein levels of SCN8A in subiculum were comparable between non-epileptic control and the pharmaco-responsive mice (the Veh group, Supporting Information Fig. S3).

For comparison, we examined $Na_v1.6$ expression in other hippocampal regions. Interestingly, $Na_v1.6$ fluorescence intensity showed specific increases in the subiculum but not in CA1, DG, or CA3 regions (Supporting Information Fig. S4A and S4B). To verify whether $Na_v1.6$ was also increased in the temporal lobe in pharmacoresistant TLE patients. We further compared the $Na_v1.6$ expression from surgically resected regions of patients with pharmacoresistant TLE (Supporting Information Table S1). As indicated in Supporting Information Fig. S5, compared with the control samples (resected regions of patients with brain glioma), the $Na_v1.6$ (*SCN8A*) protein levels in the resected hippocampal regions of pharmacoresistant TLE patients were significantly higher, suggesting a common pathological changes in both rodents and humans.

3.3. *Pharmacological $Na_v1.6$ activation in the subiculum recapitulated acquired pharmacoresistance*

Given that subicular pyramidal neuronal $Na_v1.6$ was increased in the LTG group, we asked whether activating $Na_v1.6$ would directly induce pharmacoresistance. In kindled mice from the Veh group, $Na_v1.6$ agonist VET (1 or 5 μmol/L, 0.15 μL) was intra-subicular injected, and the efficacy of LTG was tested (Fig. 3A). Fig. 3B confirms proper cannula placement in the subiculum. Electrophysiology recordings revealed that 1 μmol/L VET significantly increased I_{NaP} amplitude (Fig. 3C) and directly induced AP firings (Fig. 3D). Behavioral assessments demonstrated VET-induced pharmacoresistance in the Veh group: LTG's anticonvulsant effects on seizure stages, ADDs, and GSDs were attenuated following intra-subiculum VET administration (Fig. 3E−G). And VET dose-dependently decreased the stage lowered ratio and effective rate of LTG (Fig. 3H and I), which were further verified in the representative seizure EEGs and spectrums (Fig. 3J). However, we have noticed that VET alone only showed a tendency to prolong the ADDs in fully kindled mice of the Veh group (Fig. 3K).

Then we administrated VET during the kindling process, to test the hypothesis that pharmacological activating subicular $Na_v1.6$ could mimic acquired pharmacoresistance (Fig. 3L). The cannula position was shown in Fig. 3M. As shown in Fig. 3N and O, VET did not accelerate the progression of seizure stages and ADDs during the kindling process. However, fully kindled mice from the VET group showed pharmacoresistance to subsequent LTG tests. As LTG lost its efficacy in reducing the seizure stages, shortening the ADDs and decreasing GSDs (Fig. 3P−R). And the stage lowered ratio of LTG was significantly lower in the VET group than mice receiving saline treatments (the saline group), as well as the effective rate (Fig. 3S and T). The representative seizure EEGs and spectrums were shown in Fig. 3U. Thus, we concluded that pharmacologically activating subicular $Na_v1.6$ either during the kindling process or after fully kindled mimicked acquired pharmacoresistance.

3.4. *Subicular pyramidal neuronal $Na_v1.6$ knockdown reversed established pharmacoresistance*

Then, we administered LTG treatments to *CaMKIIα-Cre* mice during their kindling process. When they were fully kindled, *AAV-DIO-ShRNA* (*SCN8A*) or *AAV-DIO-ShRNA* (NC) were injected into the subiculum *via* the previously implanted cannula, designated as the LTG::ShRNA and the LTG::NC groups, respectively (Fig. 4A). The viruses were strictly expressed within the subiculum (Fig. 4B). Western blot analysis confirmed that *AAV-DIO-ShRNA* (*SCN8A*) effectively reduced SCN8A expression in the subiculum, compared with the control virus (Fig. 4C). The

the two group, including the threshold (I), the rise time (J), the decay time (K), the time constant value (Tau, L) and the amplitude (M) of the first AP elicited by the rheobase (*$P< 0.05$, ***$P< 0.001$, unpaired *t*-test). (N) Plot of maximal hyperpolarizing voltages reached between APs evoked by a 200 pA depolarizing current injection step (***$P< 0.001$, unpaired *t*-test). (O) Left panel: the representative traces of the membrane voltage changes in subicular pyramidal neurons under the stepped hyperpolarization currents injection from the two groups. Subicular pyramidal neurons were easily to exhibit rebound AP firings after the injection of hyperpolarization currents. Right panel: the comparison of the occurrence rate of rebound firing between the two groups (*$P< 0.05$, χ^2 test). (P) Left panel: the representative traces of the repolarization induced sag in membrane voltage after a 100 pA hyperpolarization current injection. Right panel: the comparison of the repolarization sag values between two groups after different hyperpolarization currents ($n= 15$ for the Veh group, $n= 10$ for the LTG group; *$P< 0.05$, **$P< 0.01$, ***$P< 0.001$, unpaired *t*-test). (Q) The representative activating Na^+ current traces recorded for subicular pyramidal neurons from the two groups. (R) Voltage dependence of sodium channel activation for subicular pyramidal neurons from the Veh ($n= 11$) and the LTG ($n= 12$) groups. (S) Scatter plot of voltage at half-maximal activation ($V_{1/2}$) for subicular pyramidal neurons from the two groups (**$P< 0.01$, unpaired *t*-test). (T) The comparison of the mRNA levels of each sodium channel subunit between the two groups ($n= 3$ for each group, *$P< 0.05$, unpaired *t*-test). (U) The WB examination of the $Na_v1.6$ levels in the subiculum from the two groups ($n= 3$ for each group, *$P< 0.05$, unpaired *t*-test). (V) Left panel: the representative IHC image of the $Na_v1.6$ and *CaMKIIα* co-staining in the subiculum of the two groups. Right panel: the comparison of the $Na_v1.6$ and *CaMKIIα* co-staining cells between the two groups ($n= 3$ for each group, *$P< 0.05$, unpaired *t*-test). (W) Left panel: the representative $Na_v1.6$-dependent slow-activated I_{NaP} current recorded for subicular pyramidal neurons from the two groups. Right panel: the comparison of the amplitudes of I_{NaP} between the two groups ($n= 20$ cells from 5 mice for each group, ***$P< 0.001$, unpaired *t*-test). The data are presented by mean ± SEM.

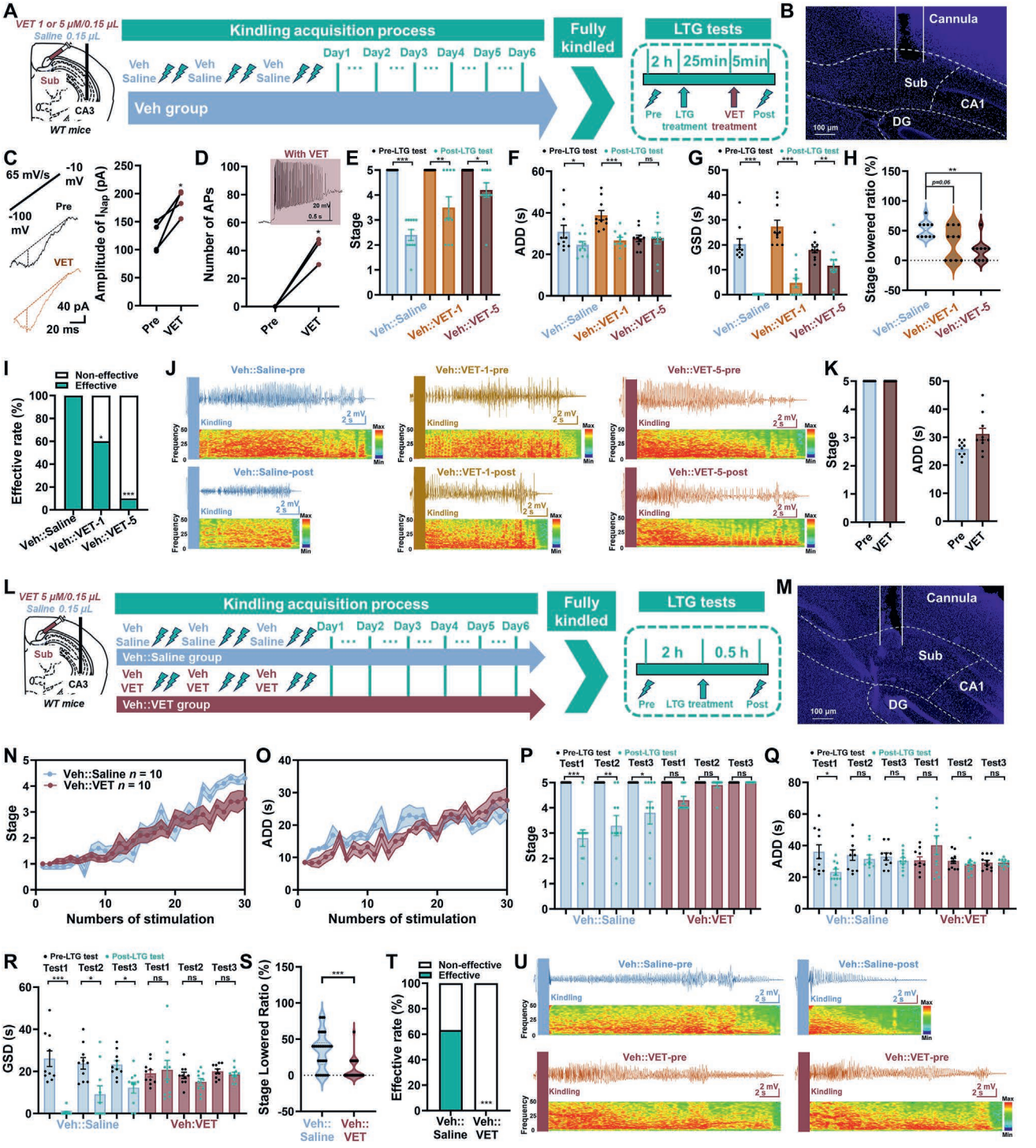

Figure 3 Pharmacological activating $Na_v1.6$ in the subiculum induces acquired pharmacoresistance. (A) The schematic of the experiments. Fully kindled mice in the Veh group received VET prior to the LTG treatment. (B) The verification of the implantation site of cannulas in the subiculum. (C) *In vitro* electrophysiological recordings of the $Na_v1.6$-mediated I_{NaP} in subicular pyramidal neurons before and after VET perfusion ($n=$ 3 cells from 2 mice, $^*P<$ 0.05, paired *t*-test). (D) The number of spontaneous APs recorded before and after VET perfusion ($n=$ 3 cells from 2 mice, $^*P<$ 0.05, paired *t*-test). (E−G) The efficacy of VET and LTG co-treatment on the seizure stages (E), ADDs (F) and GSDs (G) of the fully kindled mice from the two groups ($n=$ 10 for each group; post-LTG test *vs* pre-LTG test for each test was performed; for seizure stages, $^*P<$ 0.05, $^{**}P<$ 0.01, $^{***}P<$ 0.001, non-parametric Mann−Whitney test; for ADDs and GSDs, $^*P<$ 0.05, $^{**}P<$ 0.01, $^{***}P<$ 0.001, paired *t*-test). (H) The comparison of stage lowered ratio caused by LTG among the three groups ($^{**}P<$ 0.01, one-way ANOVA followed by Turkey's *post hoc* test). (I) The comparison of effective rate among the three groups ($^*P<$ 0.05, $^{***}P<$ 0.01, χ^2 test). (J) The representative seizure EEG and spectrums of the LTG tests of each group. (K) The effect of VET (5 μmol/L) alone on seizure stages and ADDs ($n=$ 10). (L) The schematic of the experiments. During the kindling process, Veh::VET group received vehicle and VET co-treatment. When mice

electrophysiological recordings further confirmed that subicular pyramidal neurons expressed with *AAV-DIO-ShRNA* (*SCN8A*) showed a robustly decreased I_{NaP}, and required a higher rheobase to elicit AP compared with neurons expressed the control virus (Fig. 4D and E). Behavioral results demonstrated that pharmacoresistance was fully reversed by selectively knocking down $Na_v1.6$ in subicular pyramidal neurons. Specifically, after *AAV-DIO-ShRNA* (*SCN8A*) were expressed, LTG was able to reduce the seizure stages, and shortened both ADDs and GSDs (Fig. 4F−H). Also, compared with the pre-condition, *AAV-DIO-ShRNA* (*SCN8A*) successfully raised the stage lowered ratio and the effective rate of LTG (Fig. 4I and J), as denoted by the representative seizure EEGs and spectrums (Fig. 4K). As a comparison, the expression of control virus (*AAV-DIO-ShRNA* (NC)) in subicular pyramidal neurons have no impact on acquired pharmacoresistance (Fig. 4L−Q). Then we wondered whether selectively knocking down $Na_v1.6$ in pyramidal neurons of the CA1 could also influence pharmacoresistance (Supporting Information Fig. S6A). Furthermore, we found that LTG resistance did not change even after *AAV-DIO-ShRNA* (*SCN8A*) was expressed in the CA1 (Supporting Information Fig. S6B−S6H). Taken together, these results indicated that knocking down $Na_v1.6$ in subicular pyramidal neurons successfully reversed the established acquired pharmacoresistance.

3.5. Prophylactic $Na_v1.6$ genetical inhibition in subicular pyramidal neurons prevented acquired pharmacoresistance

Given that the establishment of acquired pharmacoresistance usually requires consecutive ASM administrations, whether $Na_v1.6$ knockdown can prevent the occurrence of acquired pharmacoresistance warrant further investigation. To address this question, we conducted hippocampal kindling experiments on *CaMKIIα-Cre* mice. Specifically, mice were intra-subicular injected with either *AAV-DIO-ShRNA* (*SCN8A*) or *AAV-DIO-ShRNA* (NC), followed by combined hippocampal kindling procedure and LTG treatment (designated as LTG::NC and LTG::shRNA groups, respectively; Fig. 5A). IHC results confirmed the expression of *AAV-DIO-ShRNA* (*SCN8A*) in the subiculum (Fig. 5B). As shown in Fig. 5C and D, the progression of seizure stages and ADDs were comparable between the two groups. Notably, while LTG failed to reduce seizure stages, shorten ADDs or decrease GSDs in fully kindled mice of the LTG::NC group, *AAV-DIO-ShRNA* (*SCN8A*) restored LTG efficacy in the LTG::ShRNA group (Fig. 5E−G). Furthermore, both the stage lower ratio and effective rate of LTG were significantly higher in the LTG::ShRNA group (Fig. 5H and I). These findings, supported by representative seizure EEGs and spectrums (Fig. 5J), indicated that acquired pharmacoresistance caused by LTG administration during the kindling process was fully prevented in the LTG::ShRNA group.

Consistent with the results exhibited in Fig. 1J−O, we demonstrated that genetic inhibition of $Na_v1.6$ in subicular pyramidal neurons significantly attenuated LTG-induced pharmacoresistance in fully kindled mice. *CaMKIIα-Cre* mice which expressed *AAV-DIO-ShRNA* (*SCN8A*) in the subiculum underwent hippocampal kindling protocol with concurrent vehicle administration (Veh::ShRNA, Fig. 5K and L). Nine consecutive LTG trials were conducted post-kindling, during which LTG persistently reduced seizure stages, decreased ADDs, and shortened GSDs across all trials (Fig. 5M−O). The stage lowered ratio of LTG remained stable throughout the testing period (Fig. 5P), as evidenced by representative seizure EEGs and spectrums (Fig. 5Q). And given that refractory TLE patients exhibit resistance to multiple ASMs, we also investigated the role of genetical inhibition of subicular pyramidal neuronal $Na_v1.6$ on the genesis of multi-ASM resistance (Supporting Information Fig. S7A). Notably, *CaMKIIα-Cre* mice receiving LTG during kindling showed attenuated therapeutic responses to PHT, VPA, CBZ, RUF and LEV (Fig. S7B−S7F). However, targeted suppression of *SCN8A via* subicular administration of *AAV-DIO-shRNA* (*SCN8A*) significantly restored pharmacological sensitivity to these ASMs (Fig. S7B−S7F). Crucially, this effect exhibited cell-type specificity, as subicular GABAergic neuronal counts remain similar between pharmacoresistant and pharmaco-responsive mice (Supporting Information Fig. S8A and S8B). More importantly, early $Na_v1.6$ knockdown in subicular interneurons (injecting *AAV-DIO-ShRNA* (*SCN8A*) into *Vgat-Cre* mice) did not alter the development of acquired pharmacoresistance (Supporting Information Fig. S9A−S9J).

To further validate the hypothesis that $Na_v1.6$ knockdown in subicular pyramidal neurons prevents acquired pharmacoresistance induced by other ASMs, we performed stereotaxic injection of *AAV-DIO-ShRNA* (*SCN8A*) into the subiculum of *CaMKIIα-Cre* mice, and then kindling process along with CBZ or LEV administration were applied (Fig. 6A and K). The expression of *AAV-DIO-ShRNA* (*SCN8A*) are shown in Fig. 6B and L. Similarly, *AAV-DIO-ShRNA* (*SCN8A*) did not influence the progression of seizure stages and ADDs during kindling development (Fig. 6C, D, M and N). Interestingly, compared with the Veh::NC group (*CaMKIIα-Cre* mice injected with *AAV-DIO-ShRNA* (*SCN8A*), and treated with vehicle during kindling process), both CBZ and LEV demonstrated diminished therapeutic efficacy in kindled mice from the CBZ::NC or LEV::NC groups (*CaMKIIα-Cre* mice injected with *AAV-DIO-ShRNA* (*SCN8A*), and treated with CBZ or LEV during kindling process). Similar to the LTG administration, the subicular $Na_v1.6$ protein levels were significantly higher in CBZ::NC or the LEV::NC group, compared with their respective Veh::NC controls (Supporting Information Fig. S10), demonstrating the universal $Na_v1.6$ alteration occurring in acquired pharmacoresistance triggered by diverse ASMs. Notably, *AAV-DIO-ShRNA* (*SCN8A*) intervention successfully restored the anti-seizure effects of CBZ and LEV in CBZ::ShRNA or LEV::ShRNA groups (Fig. 6E−G, O−Q). Importantly, genetic inhibition of $Na_v1.6$ significantly enhanced the stage lower ratio and effective rate in the CBZ::ShRNA or LEV::ShRNA groups compared with

were fully kindled, LTG tests were performed. (M) The verification of cannula implantation in the subiculum. (N, O) The progression of seizure stages and ADDs during the kindling process of the two groups ($n = 10$ for each group). (P−R) The seizure stages (E), ADDs (F) and GSDs (G) before and after the LTG treatments of the fully kindled mice from the two groups ($n = 10$ for each group, post-LTG test *vs* pre-LTG test for each test was performed; for seizure stages, $^*P < 0.05$, $^{**}P < 0.01$, $^{***}P < 0.001$, non-parametric Mann−Whitney test; for ADDs and GSDs, $^*P < 0.05$, $^{***}P < 0.001$, paired *t*-test). (S) The seizure stage lowered ratio caused by LTG of the two groups ($n = 30$ LTG tests, $^{***}P < 0.001$, unpaired *t*-test). (T) The effective rate of the two groups ($^{***}P < 0.001$, χ^2 test). (U) The representative seizure EEGs and spectrums of the two groups. All data are presented by mean ± SEM.

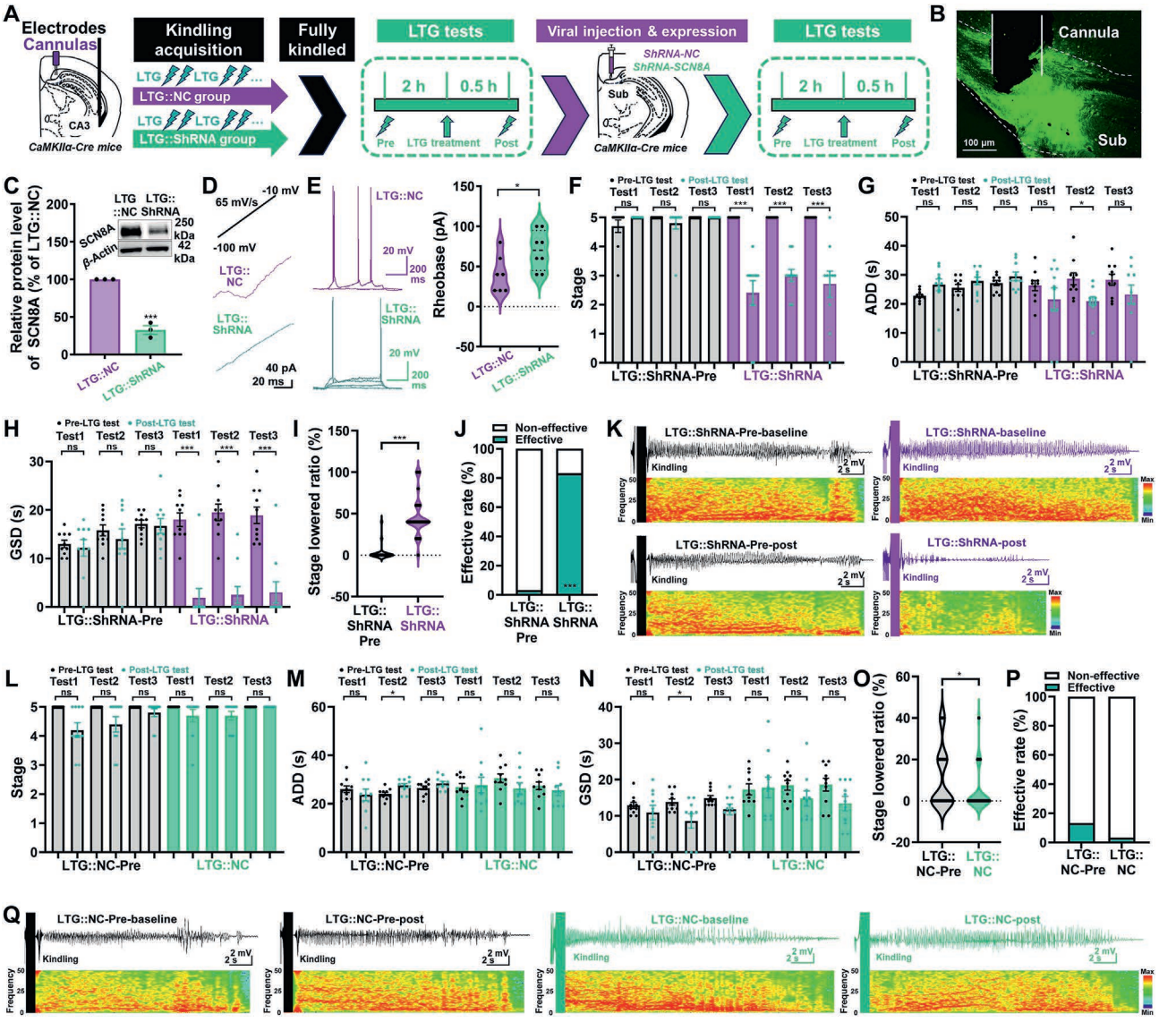

Figure 4 $Na_v1.6$ knockdown in subicular pyramidal neurons reversed acquire pharmacoresistance. (A) The schematic of the experimental design. Mice were initially under kindling acquisition along treated with LTG, when fully kindled, LTG tests were performed. Then virus was injected into the subiculum allow for expression, followed by LTG tests. (B) The histological verification of *AAV-shRNA* (*SCN8A*) expression in coronal brain slices in the subiculum. (C) The WB verification of the *AAV-shRNA* (*SCN8A*) on the subicular protein levels of $Na_v1.6$ ($n=$ 3 for each group, $***P<$ 0.001, unpaired *t*-test). (D) Patch clamp recordings of I_{NaP} in *AAV-shRNA* (*SCN8A*) and control virus transfected subicular pyramidal neurons. (E) The effect of genetical knock down $Na_v1.6$ on the excitability of subicular pyramidal neurons (Left panel: the representative trace of ap, right panel: the comparison of the rheobases between the two groups, $n=$ 7 for LTG::NC, $n=$ 8 for LTG::shRNA, $*P<$ 0.05, unpaired *t*-test). (F−H) The seizure stages (F), ADDs (G) and GSDs (H) before and after the LTG treatments of the fully kindled pharmacoresistant mice before and after ShRNA expression ($n=$ 10, post-LTG test *vs* pre-LTG test for each test was performed; for seizure stages, $***P<$ 0.001, non-parametric Mann-Whitney test; for ADDs and GSDs, $*P<$ 0.05, $***P<$ 0.001, paired *t*-test). (I) The comparison of the stage lowered ratio caused by LTG before and after the ShRNA expression ($n=$ 30 tests, $***P<$ 0.001, paired *t*-test). (J) The effective rate of LTG ($***P<$ 0.001, paired *t*-test, chi-squre test). (K) The representative seizure EEGs and spectrums. (L−N) The seizure stages (L), ADDs (M) and GSDs (N) before and after the LTG treatments of the fully kindled pharmacoresistant mice before and after control virus expression ($n=$ 10, $*P<$ 0.05, paired *t*-test). (O) The stage lowered ratio caused by LTG before and after the control virus expression ($n=$ 30 tests, $*P<$ 0.05, paired *t*-test). (P) The effective rate of LTG. (Q) The representative seizure EEGs and spectrums. The data are presented by mean ± SEM.

their respective *NC* controls (Fig. 6H, I, R, S). Representative seizure EEGs and spectrums further confirmed that knockdown of $Na_v1.6$ in subicular pyramidal neurons effectively prevented the development of acquired pharmacoresistance to both CBZ and LEV (Fig. 6J and T).

3.6. Impaired inhibition on subicular pyramidal neurons is associated with the acquired pharmacoresistance

Lastly, to preliminarily investigate the possible mechanisms underlying how increased $Na_v1.6$ in subicular pyramidal neurons

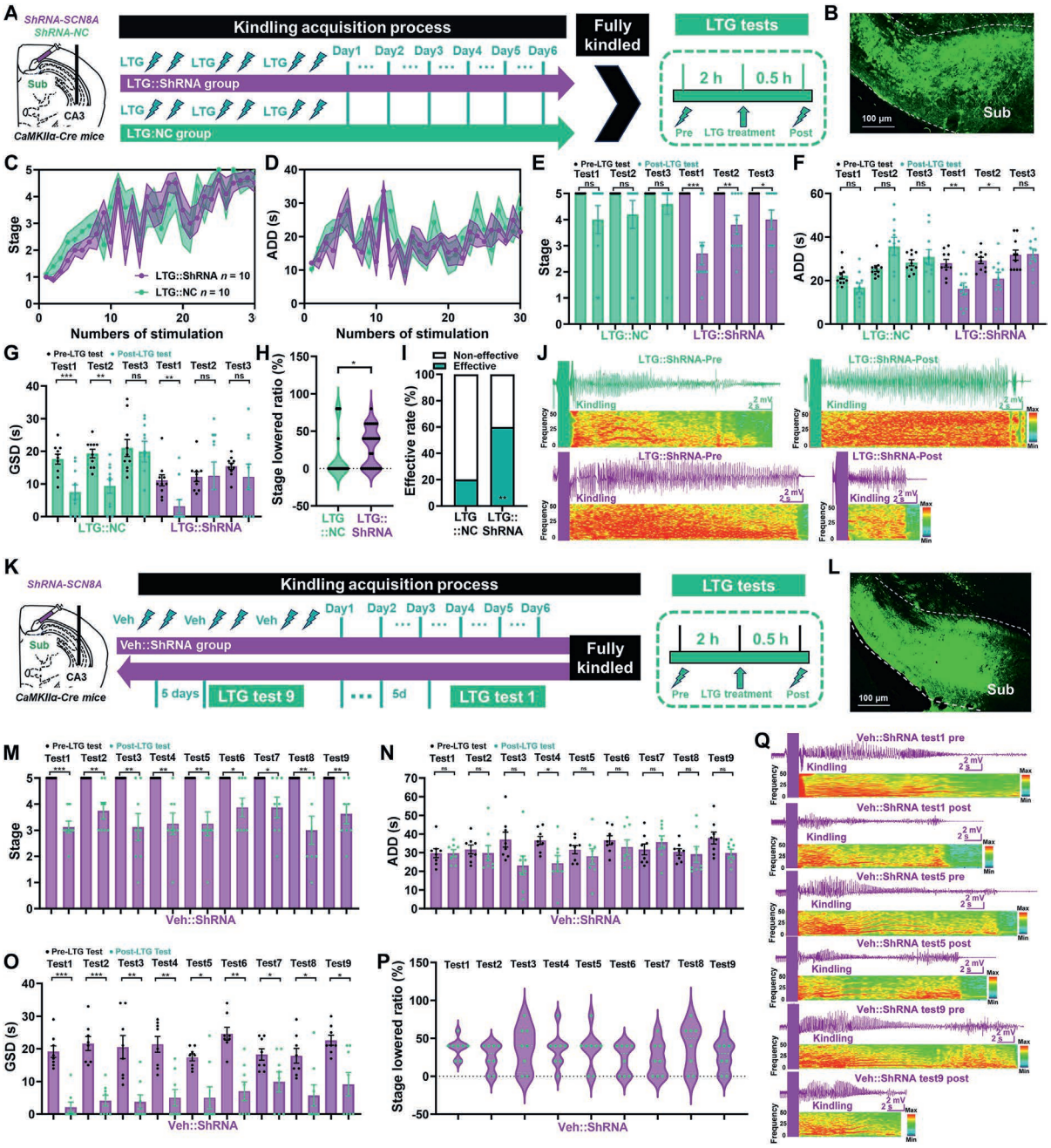

Figure 5 Early genetical interference of $Na_v1.6$ in subicular pyramidal neurons prevents the establishment of acquire pharmacoresistance. (A) The schematic of experimental design. *CaMKIIα-Cre* mice received *AAV-ShRNA* (*SCN8A*) or *AAV-ShRNA* (NC) injection into the subiculum. Then kindling process along with LTG administrations were applied. When fully kindled, the efficacy of LTG was tested on each mice. (B) The histological verification of *AAV-shRNA* (*SCN8A*) expression in coronal brain slices in the subiculum. (C, D) The progression of seizure stages and ADDs during the kindling process of the two groups ($n = 10$ for both groups). (E−G) The seizure stages (E), ADDs (F) and GSDs (G) before and after the LTG treatments of the fully kindled mice from the LTG::NC and LTG::ShRNA groups ($n = 10$ for each group, post-LTG test *vs* pre-LTG test for each test was performed; for seizure stages, $^*P < 0.05$, $^{**}P < 0.01$, $^{***}P < 0.001$, non-parametric Mann−Whitney test; for ADDs and GSDs, $^*P < 0.05$, $^{**}P < 0.01$, $^{***}P < 0.001$, paired *t*-test). (H) The seizure stage lowered ratio caused by LTG of the two groups ($n = 30$ LTG tests, $^*P < 0.05$, unpaired *t*-test). (I) The effective rate of the two groups ($^{***}P < 0.001$, χ^2 test). (J) The representative seizure EEGs and spectrums during the LTG tests of the two groups. (K) *CaMKIIα-Cre* mice were injected with *AAV-ShRNA* (*SCN8A*) into the subiculum. Then kindling process along with vehicle treatments were applied. When mice were fully kindled, a total of nine LTG tests were performed. (L) The histological verification of *AAV-shRNA* (*SCN8A*) expression in coronal brain slices in the subiculum. (M−O) The efficacy of LTG on seizure stages (M), ADDs (N) and GSDs (O) on mice from the Veh::ShRNA group ($n = 8$, post-LTG test *vs* pre-LTG test for each test was performed; for seizure stages, $^*P < 0.05$, $^{**}P < 0.01$, $^{***}P < 0.001$, non-parametric Mann−Whitney test; for ADDs and GSDs, $^*P < 0.05$, $^{**}P < 0.01$, $^{***}P < 0.001$, paired *t*-test). (P) The seizure stage lowered ratio caused by LTG of the nine LTG tests. (Q) The representative seizure EEGs and spectrums of the first, fifth, and ninth LTG tests. The data are presented by mean ± SEM.

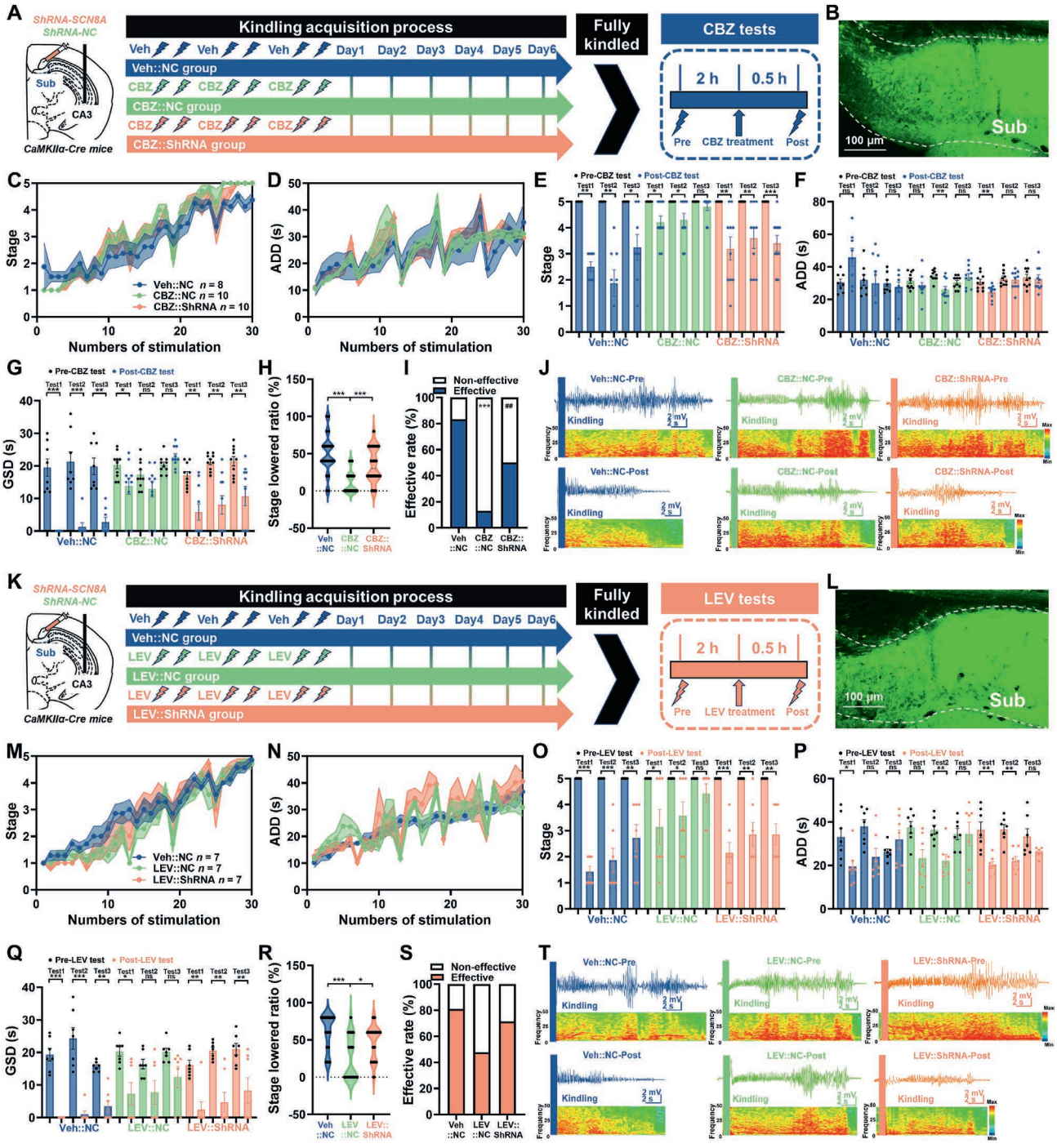

Figure 6 Early genetical interference of $Na_v1.6$ in subicular pyramidal neurons prevents the establishment of acquire pharmacoresistance caused by multiple ASMs. (A) The schematic of the experimental design. *AAV-ShRNA* (*SCN8A*) or *AAV-ShRNA* (NC) were injected into the subiculum of *CaMKIIα-Cre* mice. Then mice were treated with CBZ or vehicle during the kindling process. When fully kindled, the efficacy of CBZ was tested. (B) The histological verification of *AAV-shRNA* (*SCN8A*) expression in coronal brain slices in the subiculum. (C, D) The progression of seizure stages and ADDs during the kindling process of the three groups ($n=$ 8 for Veh::NC group, $n=$ 10 for CBZ::NC and CBZ::ShRNA groups). (E−G) The efficacy of CBZ on the seizure stages (E), ADDs (F) and GSDs (G) on the fully kindled mice from each group ($n=$ 8 for Veh::NC group, $n=$ 10 for CBZ::NC and CBZ::ShRNA groups; for seizure stages, $^*P<$ 0.05, $^{**}P<$ 0.01, non-parametric Mann−Whitney test; for ADDs and GSDs, $^*P<$ 0.05, $^{**}P<$ 0.01, $^{***}P<$ 0.001, paired *t*-test). (H) The seizure stage lowered ratio caused by CBZ of the three groups ($n=$ 24 LTG tests for Veh::NC group, $n=$ 30 for CBZ::NC and CBZ::ShRNA groups; $^{***}P<$ 0.001, one-way ANOVA followed by Turker *post hoc* test). (I) The comparison of the effective rate of CBZ among three groups ($^{***}P<$ 0.001, compared with the Veh::NC group; $^{\#\#}P<$ 0.01, compared with the CBZ::NC group; χ^2 test). (J) The representative seizure EEGs and spectrums. (K) The schematic of the experimental design in testing the efficacy of *AAV-ShRNA* (*SCN8A*) on LEV induced acquired pharmacoresistance. (L) The histological verification of *AAV-shRNA* (*SCN8A*) expression in coronal brain slices in the subiculum. (M, N) The progression of seizure stages and ADDs during the

induce pharmacoresistance, we conducted *in vitro* electrophysiological recordings in kindled mice from the Veh, the LTG and the LTG::shRNA groups (Fig. 7A). As expected, LTG effectively reduced the number of APs elicited by each depolarized current in the Veh group (Fig. 7B). However, this characteristic inhibition on neuronal excitability was completely abolished in neurons from the LTG group, demonstrating an acquired resistance mechanism (Fig. 7C). Consequently, the rate of APs numbers during the LTG administration was significantly elevated in the LTG group, regardless of the intensity of depolarized currents (Fig. 7D). Furthermore, while LTG administration effectively increased the rheobase (the minimum current required to elicit APs) in the Veh group, this electrophysiological parameter remained unchanged in the LTG group (Fig. 7E), resulting in a markedly lower rheobase increased ratio in the LTG group (Fig. 7F). Considering that sodium channel inhibitor like LTG primarily suppress neuronal synchronization through membrane stabilization, we observed that LTG induced a hyperpolarizing shift in the resting membrane potential (RMP) of subicular pyramidal neurons in the Veh group. Notably, this electrophysiological modification was absent in neurons from the LTG group (Fig. 7G). Consequently, the magnitude of RMP difference before and after LTG administration was significantly attenuated in the LTG group (Fig. 7H).

Subsequent experiments evaluated whether chemogenetic potentiation of inhibitory effects on subicular pyramidal neurons could reverse acquired pharmacoresistance (Fig. 7I). Following precise *AAV-Dio-hm4di-mCherry* expression in the subiculum (Fig. 7J), comparative analysis revealed that chemogenetic inhibition of subicular pyramidal neurons significantly reversed pharmacoresistance in LTG::hm4di mice compared to LTG::mCherry controls (Fig. 7K−M). It can be observed that mice from the LTG::mCherry group exhibited pharmacoresistance to Clozapine *N*-oxide (CNO) and LTG co-treatment, in identical to the modeling results shown in previous results. While CNO and LTG co-treatment effectively reduced the seizure stages, shortened ADDs and GSDs in mice from the LTG::hm4di group. Also, the stage lowered ratio and effective rate were significantly higher in the LTG::hm4di group (Fig. 7N and O), which was denoted in the representative seizure EEGs (Fig. 7P). These results suggested that specifically inhibition of subicular pyramidal neurons by chemogenetics effectively reversed pharmacoresistance. However, CNO monotherapy only marginally affected the seizure stages and raised the stage lowered ratio in mice from the LTG::hm4di group, but have no impact on the LTG::mCherry group (Fig. 7Q−T). Collectively, these findings demonstrated that impaired LTG-mediated inhibition of subicular pyramidal neurons underlies acquired pharmacoresistance mechanisms.

4. Discussion

While innate pharmacoresistance can be rapidly identified upon initial ASM administration, acquired pharmacoresistance typically emerges following prolonged effective treatments[7]. The distinct phenotypic manifestations of these pharmacoresistant states suggest divergent pathophysiological mechanisms. Notably, the classical "transporter hypothesis" may provide an incomplete explanation for acquired pharmacoresistance, as transporter abnormalities from genetic polymorphisms primarily contribute to intrinsic pharmacoresistance during initial ASM exposure[30], while the mechanistic theories for acquired pharmacoresistance remain scarce. Our investigation revealed that acquired pharmacoresistance in TLE stems from subicular pyramidal neuron hyperexcitability mediated by $Na_v1.6$ upregulation. This mechanism fundamentally differs from *SCN8A* gain-of-function mutation-induced developmental epileptic encephalopathies[17]. Unlike previous studies demonstrating $Na_v1.6$'s seizure-modulating effects in global brain networks[29,31-33], our findings establish that region-specific $Na_v1.6$ dysregulation in subicular pyramidal neurons primarily mediates pharmacoresistance rather than influencing ictogenesis. Previous investigations have implicated VGSC β-subunits (unaltered in our model) in ASM resistance[34-36]. However, such resistance appears limited to sodium channel blockers in those contexts, likely due to β-subunit modulation of drug-binding sites within VGSCs' intracellular S6 segments[37,38]. Crucially, our study reveals that $Na_v1.6$-driven subicular hyperexcitability induces broad-spectrum resistance encompassing ASMs with diverse mechanisms (*e.g.*, LEV). This finding aligns with clinical observations correlating seizure network hyperexcitability with multi-ASM resistance[39], while emphasizing the key insights: (1) the topographic specialization of $Na_v1.6$ in pharmacoresistant TLE circuitry, and (2) its unique role in mediating acquired pharmacoresistance across multiple ASM classes. Given that the subicular $Na_v1.6$ is vulnerable and seizure-susceptible in TLE[19], as well as the subiculum's limbic-specific role as the dominant hippocampal output[10], this mechanism may exhibit TLE-selective relevance. Its unique biophysical properties—including low activation threshold and functional modulation of sodium-activated potassium channels to accelerate repolarization—not only enhance neuronal excitability but also promote stronger recovery from hyperpolarization, thereby sustaining high-frequency firing[19,29,40]. Future studies need further test the generalizability to other epilepsy types (*e.g.*, neocortical epilepsy) of $Na_v1.6$ mediated mechanisms in pharmacoresistance where hippocampal-subicular circuits are less implicated.

Notably, repetitive ASM administration during epileptogenesis selectively induced pronounced $Na_v1.6$ upregulation localized to the subiculum. We propose that this regional specificity stems from the subiculum's unique pathophysiological role in TLE[10,41,42]. Our previous work demonstrated that subicular pyramidal neurons serve as critical mediators of seizure generalization by propagating hippocampal hyperexcitability to thalamocortical circuits[12]. Within this mechanistic framework, ASM efficacy in TLE mice primarily depends on suppressing seizure generalization—a process governed by subicular projection neuron hyperexcitability[43]. In this study, we further preliminary examined the role of subicular GABAergic neurons which control seizure generalization *via* activity-dependent chloride dysregulation[44], they exhibit limited influence on

kindling process of the three groups ($n = 7$ for each group). (E−G) The efficacy of LEV on the seizure stages (O), ADDs (P) and GSDs (Q) on the fully kindled mice from each group ($n = 7$ for each group; for seizure stages, $^*P < 0.05$, $^{**}P < 0.01$, $^{***}P < 0.001$, non-parametric Mann−Whitney test; for ADDs and GSDs, $^*P < 0.05$, $^{**}P < 0.01$, $^{***}P < 0.001$, paired *t*-test). (R) The seizure stage lowered ratio caused by LEV of the three groups ($n = 21$ LTG tests for each group; $^*P < 0.05$, $^{***}P < 0.001$, one-way ANOVA followed by Turker *post hoc* test). (S) The comparison of the effective rate of LEV among three groups. (T) The representative seizure EEGs and spectrums. The data are presented by mean ± SEM.

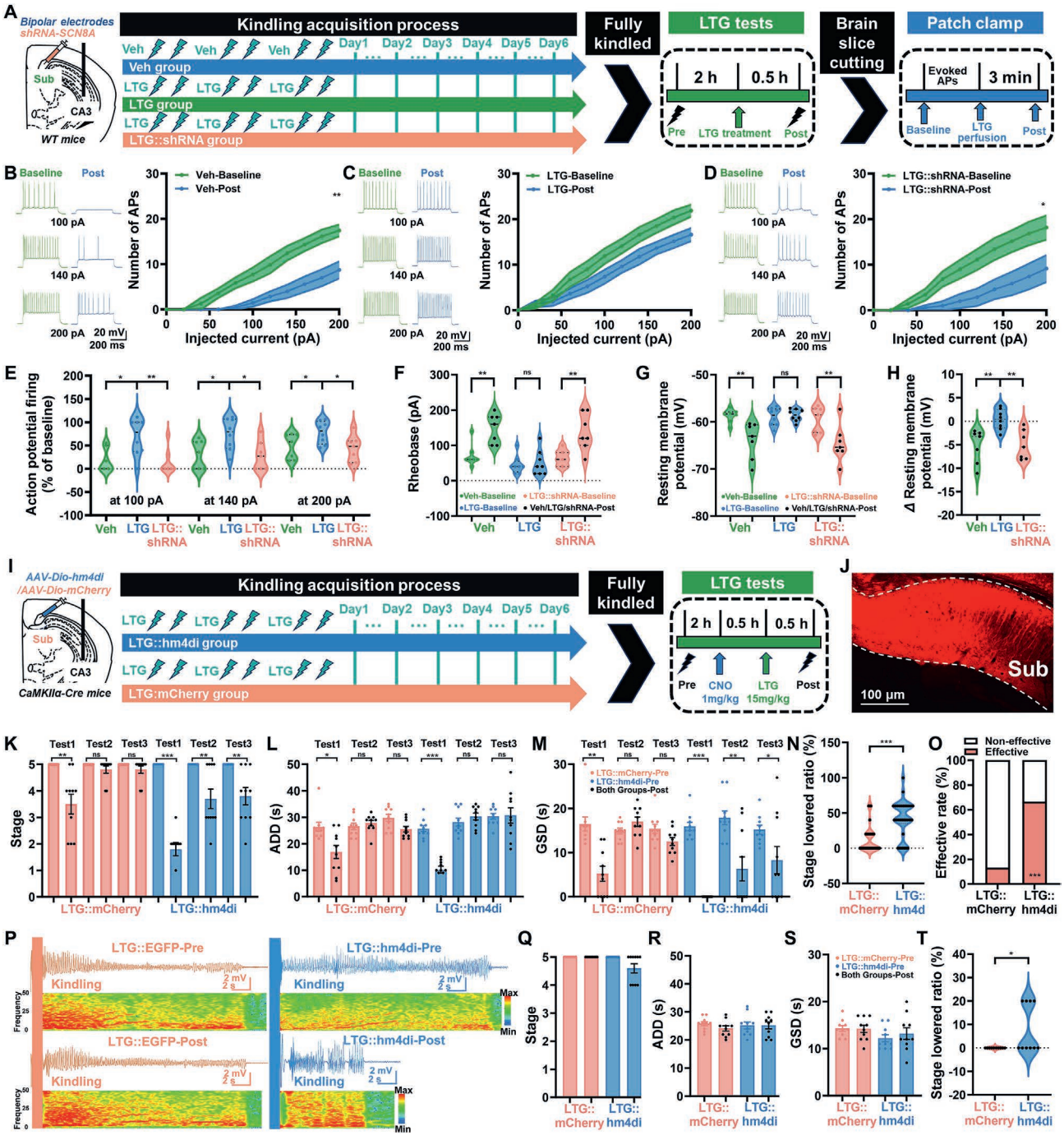

Figure 7 Compensatory increases in $Na_v1.6$ offsetting LTG's blockade on action potentials of subicular pyramidal neurons is responsible for the acquired pharmacoresistance. (A) The process schematic of the electrophysiological experiment, fully kindled mice from the Veh, the LTG and the LTG::shRNA groups were under electrophysiological recordings on subicular pyramidal neurons. (B) The efficacy of LTG on the evoked AP firings on subicular pyramidal neurons from fully kindled mice of the Veh group. Left panel: the representative traces of AP firings elicited by different depolarized currents injection before/after LTG perfusion. Right panel: the efficacy of LTG on the numbers of APs elicited by stepped depolarized currents ($n = 7$ cells from 3 mice, $^{**}P < 0.01$, two-way ANOVA tests). (C) The efficacy of LTG on the evoked AP firings on subicular pyramidal neurons from fully kindled mice of the LTG group. Left panel: the representative traces of AP firings elicited by different depolarized currents injection before/after LTG perfusion. Right panel: the efficacy of LTG on the numbers of APs elicited by stepped depolarized currents ($n = 8$ cells from 3 mice). (D) The efficacy of LTG on the evoked AP firings on subicular pyramidal neurons from fully kindled mice of the LTG::shRNA group. Left panel: the representative traces of AP firings elicited by different depolarized currents injection before/after LTG perfusion. Right panel: the efficacy of LTG on the numbers of APs elicited by stepped depolarized currents ($n = 7$ cells from 3 mice, $^{*}P < 0.05$, two-way ANOVA tests). (E) Comparison of the AP percentage to the baseline under different depolarized stepped current injections ($^{*}P < 0.05$, $^{**}P < 0.01$, one-way ANOVA test). (F) The comparison of rheobase currents before and after LTG perfusion in the three groups ($^{**}P < 0.01$, paired *t*-test). (G) The comparison of the resting membrane potentials before and after LTG perfusion ($^{**}P < 0.01$, paired *t*-test). (H) The

pharmacoresistance for three possible reasons: (1) Their interneuron identity restricts function to local excitatory-inhibitory (E/I) balance, unlike pyramidal neurons that propagate seizures *via* long-range projections; (2) GABAergic dysfunction (depolarizing shift) primarily enables secondary generalization—a process occurred preceding pharmacoresistance in current kindling model; and (3) First-line ASMs mainly aimed to inhibit pyramidal neurons, whose maladaptive $Na_v1.6$ upregulation directly undermines therapeutic efficacy. Thus, acquired pharmacoresistance represents a distinct pathophysiological state driven by this vulnerability of pyramidal neurons. Given the $Na_v1.6$'s preferential enrichment in the AIS of subicular pyramidal neurons[19,45], we propose the following pathogenic cascade: while ASMs initially suppress seizure generalization, residual paroxysmal activity from epileptic foci continues to drive subicular neuronal firing. This persistent activation drives activity-dependent axonal $Na_v1.6$ upregulation (consistent with this VGSC isoform's known activity-dependent plasticity)[33,46], establishing a maladaptive feedback loop that progressively diminishes ASM efficacy. This upregulation likely attenuates the effect ASMs such as lamotrigine—that primarily targets fast activated VGSCs—through compensatory increases in $Na_v1.6$'s slow and sustained activation, thereby sustaining neuronal excitability despite sodium channel blockade. We have not yet elucidated the specific signaling pathways, transcriptional regulators, or post-transcriptional modifications responsible for the increased $Na_v1.6$ expression following repeated ASM exposure. Unraveling these mechanisms is a critical direction for future research. Specifically, $Na_v1.6$ upregulation compromises inhibitory control over subicular pyramidal neuron excitability, thereby establishing a pharmacoresistant state. Critically, these findings extend our prior discovery of caspase-1-mediated innate pharmacoresistance in the subiculum[13], collectively positioning this structure as a pivotal "gate" for divergent TLE pharmacoresistance mechanisms: innate resistance *via* neuroinflammatory pathways versus acquired resistance through activity-dependent ion channel remodeling.

Current therapeutic options for pharmacoresistant TLE remain limited by insufficient molecular targets[2,47]. In response to this clinical challenge, recent pharmacological advances have focused on developing novel ASMs with improved efficacy against refractory epilepsy[48-50]. Emerging clinical evidence demonstrates enhanced therapeutic effects of newly approved ASMs with innovative mechanisms in specific epilepsy syndromes, including mTOR inhibitors like everolimus for tuberous sclerosis complex-related epilepsy and cannabidiol for Lennox-Gastaut/Dravet syndromes[51,52]. For acquired pharmacoresistant TLE, our findings demonstrate that genetic $Na_v1.6$ ablation in subicular pyramidal neurons restores conventional ASM efficacy. Crucially, prolonged ASM administration failed to induce acquired pharmacoresistance in mice with prophylactic $Na_v1.6$ suppression, providing the first preclinical evidence that $Na_v1.6$ inhibition constitutes a dual-purpose strategy for both treating and preventing acquired pharmacoresistance. Currently available sodium channel-blocking ASMs primarily target fast-activated sodium channel subunits ($Na_v1.1$ and $Na_v1.2$)[53,54]. Although no selective $Na_v1.6$ inhibitor is currently approved, promising candidates like zandatrigine are undergoing Phase II trials[55]. Investigating these compounds in patients developing pharmacoresistance following long-term ASM treatment could open new therapeutic avenues.

5. Conclusions

This study demonstrates that subicular pyramidal neuron $Na_v1.6$ upregulation drives acquired pharmacoresistance in TLE. These findings advance our mechanistic understanding of epilepsy pharmacoresistance while establishing $Na_v1.6$ as a compelling dual-purpose target for managing and preventing pharmacoresistant TLE.

Acknowledgments

This work was supported by grants from the National Natural Science Foundation of China (Nos. 82173796, 82374064, and 82330116), the Natural Science Foundation of Zhejiang Province (Nos. LQ22H310003 and LD24H310001), and the Research Project of Zhejiang Chinese Medical University (2023JKZDZC04, China).

Author contributions

Yuanzhi Yang: Methodology, Investigation, Formal analysis, Writing - original draft. Menghan Li: Methodology, Investigation, Formal analysis. Minjuan Sun: Methodology, Investigation, Formal analysis. Shuo Zhang: Methodology, Investigation. Xiongfeng Guo: Methodology, Investigation. Shuangshuang Wu: Methodology, Investigation. Yiwei Gong: Methodology, Investigation. Lan Huang: Methodology, Investigation. Tong Liu: Methodology, Investigation. Junxiu Ye: Methodology, Investigation. Xiangyu Ma: Methodology, Investigation. Xiaoyun Qiu: Methodology, Investigation. Shuang Wang: Methodology, Investigation. Fan Fei: Methodology, Investigation. Yu Du: Writing − review & editing. Yi Wang: Writing − review & editing. Zhong Chen: Writing − review & editing, Supervision, Project administration, Funding acquisition. Cenglin Xu: Conceptualization,

comparison of difference value of resting membrane potential caused by the LTG (**$P< 0.01$, one-way ANOVA test). (I) The schematic of the chemogenetic experiments. *CaMKIIα-Cre* mice were injected with chemogenetic virus *AAV-DIO-hm4di* or *AAV-DIO-mCherry* (as control). Then kindling process along with LTG treatments were performed. When mice were fully kindled, CNO and LTG co-treatments was administrated. (J) The histological verification of *AAV-DIO-hm4di* expression in coronal brain slices in the subiculum. (K−M) The efficacy of CNO and LTG co-treatments on seizure stages (K), ADDs (L) and GSDs (M) on mice from the LTG::mCherry and LTG::hm4di groups ($n= 10$ for each group, pos *vs* pre for each test was performed; for seizure stages, **$P< 0.01$, ***$P< 0.001$, non-parametric Mann−Whitney test; for ADDs and GSDs, *$P< 0.05$, **$P< 0.01$, ***$P< 0.001$, paired t-test). (N) The seizure stage lowered ratio caused by LTG and CNO co-treatment ($n= 30$ tests, ***$P< 0.001$, unpaired *t*-test). (O) Comparative treatment efficacy between the two groups (***$P< 0.001$, χ^2 test). (P) The representative seizure EEGs and spectrums during the LTG and CNO co-treatments of the two groups. (Q−S) The efficacy of CNO along on the seizure stages (Q), ADDs (R) and GSDs (S) of mice from LTG:mCherry and LTG::hm4di groups ($n= 10$ for each group). (T) The seizure stage lowered ratio caused by CNO ($n= 10$ tests, *$P< 0.05$, unpaired *t*-test). The data are presented by mean ± SEM.

Writing − review & editing, Supervision, Project administration, Funding acquisition.

Study approval

All animal study procedures were approved by the Institutional Animal Care and Use Committee (IACUC) of Zhejiang Chinese Medical University (Approval No. 20230306-10) following ARRIVE guidelines. The clinical study was approved by the Ethics Committees of the Second Affiliated Hospital, School of Medicine, Zhejiang University (approval number: 2021-0012), and carried out in accordance with The Code of Ethics of the World Medical Association (Declaration of Helsinki) for experiments involving humans. Informed consent was obtained for experimentation with human subjects.

Conflicts of interest

The authors declare no conflicts of interest.

Appendix A. Supporting information

Supporting information to this article can be found online at https://doi.org/10.1016/j.apsb.2026.04.011.

References

1. Collaborators GBDE. Global, regional, and national burden of epilepsy, 1990−2021: a systematic analysis for the Global Burden of Disease Study 2021. *Lancet Public Health* 2025;**10**:e203−27.
2. Xu C, Gong Y, Wang Y, Chen Z. New advances in pharmacoresistant epilepsy towards precise management-from prognosis to treatments. *Pharmacol Ther* 2022;**233**:108026.
3. Kalilani L, Sun X, Pelgrims B, Noack-Rink M, Villanueva V. The epidemiology of drug-resistant epilepsy: a systematic review and meta-analysis. *Epilepsia* 2018;**59**:2179−93.
4. Berg AT, Langfitt J, Shinnar S, Vickrey BG, Sperling MR, Walczak T, et al. How long does it take for partial epilepsy to become intractable?. *Neurology* 2003;**60**:186−90.
5. Geerts A, Brouwer O, Stroink H, van Donselaar C, Peters B, Peeters E, et al. Onset of intractability and its course over time: the Dutch study of epilepsy in childhood. *Epilepsia* 2012;**53**:741−51.
6. Ekman FR, González-Martínez JA. Insular epilepsy: functions, diagnostic approaches, and surgical interventions. *J Integr Neurosci* 2024; **23**:209.
7. Berg AT, Vickrey BG, Testa FM, Levy SR, Shinnar S, DiMario F, et al. How long does it take for epilepsy to become intractable? A prospective investigation. *Ann Neurol* 2006;**60**:73−9.
8. Xu C, Wang Y, Zhang S, Nao J, Liu Y, Wang Y, et al. Subicular pyramidal neurons gate drug resistance in temporal lobe epilepsy. *Ann Neurol* 2019;**86**:626−40.
9. Perucca E, Perucca P, White HS, Wirrell EC. Drug resistance in epilepsy. *Lancet Neurol* 2023;**22**:723−34.
10. Fei F, Wang X, Wang Y, Chen Z. Dissecting the role of subiculum in epilepsy: research update and translational potential. *Prog Neurobiol* 2021;**201**:102029.
11. Cohen I, Navarro V, Clemenceau S, Baulac M, Miles R. On the origin of interictal activity in human temporal lobe epilepsy *in vitro*. *Science* 2002;**298**:1418−21.
12. Fei F, Wang X, Xu C, Shi J, Gong Y, Cheng H, et al. Discrete subicular circuits control generalization of hippocampal seizures. *Nat Commun* 2022;**13**:5010.
13. Xu C, Zhang S, Gong Y, Nao J, Shen Y, Tan B, et al. Subicular caspase-1 contributes to pharmacoresistance in temporal lobe epilepsy. *Ann Neurol* 2021;**90**:377−90.
14. Zhong K, Wu DC, Jin MM, Xu ZH, Wang Y, Hou WW, et al. Wide therapeutic time-window of low-frequency stimulation at the subiculum for temporal lobe epilepsy treatment in rats. *Neurobiol Dis* 2012;**48**:20−6.
15. Fei F, Wang X, Fan X, Gong Y, Yang L, Wang Y, et al. Circuit reorganization of subicular cell-type-specific interneurons in temporal lobe epilepsy. *J Neurosci* 2025;**45**:e0760242024.
16. de Lera Ruiz M, Kraus RL. Voltage-gated sodium channels: structure, function, pharmacology, and clinical indications. *J Med Chem* 2015; **58**:7093−118.
17. Meisler MH. SCN8A encephalopathy: mechanisms and models. *Epilepsia* 2019;**60**(Suppl 3):S86−91.
18. Blumenfeld H, Lampert A, Klein JP, Mission J, Chen MC, Rivera M, et al. Role of hippocampal sodium channel Nav1.6 in kindling epileptogenesis. *Epilepsia* 2009;**50**:44−55.
19. Barker BS, Nigam A, Ottolini M, Gaykema RP, Hargus NJ, Patel MK. Pro-excitatory alterations in sodium channel activity facilitate subiculum neuron hyperexcitability in temporal lobe epilepsy. *Neurobiol Dis* 2017;**108**:183−94.
20. Ruan Y, Xu C, Lan J, Nao J, Zhang S, Fan F, et al. Low-frequency stimulation at the subiculum is anti-convulsant and anti-drug-resistant in a mouse model of lamotrigine-resistant temporal lobe epilepsy. *Neurosci Bull* 2020;**36**:654−8.
21. Chen B, Xu C, Wang Y, Lin W, Wang Y, Chen L, et al. A disinhibitory nigra-parafascicular pathway amplifies seizure in temporal lobe epilepsy. *Nat Commun* 2020;**11**:923.
22. Wang Y, Wang Y, Xu C, Wang S, Tan N, Chen C, et al. Direct septum-hippocampus cholinergic circuit attenuates seizure through driving somatostatin inhibition. *Biol Psychiatry* 2020;**87**:843−56.
23. Racine RJ. Modification of seizure activity by electrical stimulation. II. Motor seizure. *Electroencephalogr Clin Neurophysiol* 1972;**32**: 281−94.
24. Postma T, Krupp E, Li XL, Post RM, Weiss SRB. Lamotrigine treatment during amygdala-kindled seizure development fails to inhibit seizures and diminishes subsequent anticonvulsant efficacy. *Epilepsia* 2000;**41**:1514−21.
25. Metcalf CS, Huff J, Thomson KE, Johnson K, Edwards SF, Wilcox KS. Evaluation of antiseizure drug efficacy and tolerability in the rat lamotrigine-resistant amygdala kindling model. *Epilepsia Open* 2019;**4**:452−63.
26. Yan MQ, Qiu XY, Zhang S, Yu XM, Sun MJ, Yang YZ, et al. Neuroinflammation leads to pharmacoresistance in temporal lobe epilepsy *via* promoting spermine degradation. *Acta Pharmacol Sin* 2025;**46**:2908−23.
27. Zhu HL, Wassall RD, Takai M, Morinaga H, Nomura M, Cunnane TC, et al. Actions of veratridine on tetrodotoxin-sensitive voltage-gated Na currents, Na1.6, in murine vas deferens myocytes. *Br J Pharmacol* 2009;**157**:1483−93.
28. Srivastava AK, Alex AB, Wilcox KS, White HS. Rapid loss of efficacy to the antiseizure drugs lamotrigine and carbamazepine: a novel experimental model of pharmacoresistant epilepsy. *Epilepsia* 2013;**54**: 1186−94.
29. Liu Y, Lai S, Ma W, Ke W, Zhang C, Liu S, et al. CDYL suppresses epileptogenesis in mice through repression of axonal Nav1.6 sodium channel expression. *Nat Commun* 2017;**8**:355.
30. Czornyj L, Auzmendi J, Lazarowski A. Transporter hypothesis in pharmacoresistant epilepsies. Is it at the central or peripheral level?. *Epilepsia Open* 2022;**7**(Suppl 1):S34−46.
31. Oliva M, Berkovic SF, Petrou S. Sodium channels and the neurobiology of epilepsy. *Epilepsia* 2012;**53**:1849−59.
32. Hargus NJ, Nigam A, Bertram 3rd EH, Patel MK. Evidence for a role of Nav1.6 in facilitating increases in neuronal hyperexcitability during epileptogenesis. *J Neurophysiol* 2013;**110**:1144−57.
33. Sanchez Trivino CA, Spelat R, Spada F, D'Angelo C, Manini I, Rolle IG, et al. Exosomal TNF-alpha mediates voltage-gated Na^+

channel 1.6 overexpression and contributes to brain tumor-induced neuronal hyperexcitability. *J Clin Investig* 2024;**134**.
34. Uebachs M, Opitz T, Royeck M, Dickhof G, Horstmann MT, Isom LL, et al. Efficacy loss of the anticonvulsant carbamazepine in mice lacking sodium channel beta subunits *via* paradoxical effects on persistent sodium currents. *J Neurosci* 2010;**30**:8489−501.
35. Uebachs M, Albus C, Opitz T, Isom L, Niespodziany I, Wolff C, et al. Loss of beta1 accessory Na^+ channel subunits causes failure of carbamazepine, but not of lacosamide, in blocking high-frequency firing *via* differential effects on persistent Na^+ currents. *Epilepsia* 2012;**53**: 1959−67.
36. Lin CH, Ho CJ, Lu YT, Tsai MH. Response to sodium channel blocking antiseizure medications and coding polymorphisms of sodium channel genes in taiwanese epilepsy patients. *BMC Neurol* 2021; **21**:367.
37. Ragsdale DS, McPhee JC, Scheuer T, Catterall WA. Common molecular determinants of local anesthetic, antiarrhythmic, and anticonvulsant block of voltage-gated Na^+ channels. *Proc Natl Acad Sci U S A* 1996;**93**:9270−5.
38. Ragsdale DS, McPhee JC, Scheuer T, Catterall WA. Molecular determinants of state-dependent block of Na^+ channels by local anesthetics. *Science* 1994;**265**:1724−8.
39. Janmohamed M, Brodie MJ, Kwan P. Pharmacoresistance—Epidemiology, mechanisms, and impact on epilepsy treatment. *Neuropharmacology* 2020;**168**:107790.
40. Yuan T, Wang Y, Jin Y, Yang H, Xu S, Zhang H, et al. Coupling of slack and Na(V)1.6 sensitizes slack to quinidine blockade and guides anti-seizure strategy development. *eLife* 2024;**12**. RP87559.
41. Levesque M, Avoli M. The subiculum and its role in focal epileptic disorders. *Rev Neurosci* 2021;**32**:249−73.
42. Stafstrom CE. The role of the subiculum in epilepsy and epileptogenesis. *Epilepsy Curr* 2005;**5**:121−9.
43. Benini R, Avoli M. Rat subicular networks gate hippocampal output activity in an *in vitro* model of limbic seizures. *J Physiol* 2005;**566**:885−900.
44. Wang Y, Xu C, Xu Z, Ji C, Liang J, Wang Y, et al. Depolarized GABAergic signaling in subicular microcircuits mediates generalized seizure in temporal lobe epilepsy. *Neuron* 2017;**95**:92−105.e5.
45. Hu W, Tian C, Li T, Yang M, Hou H, Shu Y. Distinct contributions of Na(v)1.6 and Na(v)1.2 in action potential initiation and backpropagation. *Nat Neurosci* 2009;**12**:996−1002.
46. Ding HH, Zhang SB, Lv YY, Ma C, Liu M, Zhang KB, et al. TNF-alpha/STAT3 pathway epigenetically upregulates Nav1.6 expression in DRG and contributes to neuropathic pain induced by L5-VRT. *J Neuroinflammation* 2019;**16**:29.
47. Zhang S, Xie S, Zheng Y, Chen Z, Xu C. Current advances in rodent drug-resistant temporal lobe epilepsy models: hints from laboratory studies. *Neurochem Int* 2024;**174**:105699.
48. Loscher W, Potschka H, Sisodiya SM, Vezzani A. Drug resistance in epilepsy: clinical impact, potential mechanisms, and new innovative treatment options. *Pharmacol Rev* 2020;**72**:606−38.
49. Loscher W, Klein P. The pharmacology and clinical efficacy of antiseizure medications: from bromide salts to cenobamate and beyond. *CNS Drugs* 2021;**35**:935−63.
50. Jiang C, Yu Y, Liu J, Jiang J. Modulating inflammatory prostaglandin E2 signaling to mitigate neurobehavioral comorbidities associated with seizure disorders. *Acta Pharm Sin B* 2025;**15**:2351−62.
51. Curatolo P, Franz DN, Lawson JA, Yapici Z, Ikeda H, Polster T, et al. Adjunctive everolimus for children and adolescents with treatment-refractory seizures associated with Tuberous sclerosis complex: *post-hoc* analysis of the phase 3 EXIST-3 trial. *Lancet Child Adolesc Health* 2018;**2**:495−504.
52. Lattanzi S, Trinka E, Striano P, Rocchi C, Salvemini S, Silvestrini M, et al. Highly purified cannabidiol for epilepsy treatment: a systematic review of epileptic conditions beyond Dravet syndrome and lennox-gastaut syndrome. *CNS Drugs* 2021;**35**:265−81.
53. Mantegazza M, Curia G, Biagini G, Ragsdale DS, Avoli M. Voltage-gated sodium channels as therapeutic targets in epilepsy and other neurological disorders. *Lancet Neurol* 2010;**9**:413−24.
54. Catterall WA. Voltage-gated sodium channels at 60: structure, function and pathophysiology. *J Physiol* 2012;**590**:2577−89.
55. Johnson JP, Focken T, Khakh K, Tari PK, Dube C, Goodchild SJ, et al. NBI-921352, a first-in-class, $Na_V1.6$ selective, sodium channel inhibitor that prevents seizures in Scn8a gain-of-function mice, and wild-type mice and rats. *eLife* 2022;**11**:e72468.